ANESTHESIOLOGY

Changes in Whole Brain Dynamics and Connectivity Patterns during Sevoflurane- and Propofol-induced Unconsciousness Identified by Functional Magnetic Resonance Imaging

Daniel Golkowski, M.D., Stephen Karl Larroque, M.A., Audrey Vanhaudenhuyse, Ph.D., Alain Plenevaux, Ph.D., Melanie Boly, M.D., Ph.D., Carol Di Perri, M.D., Ph.D., Andreas Ranft, M.D., Gerhard Schneider, M.D., Steven Laureys, M.D., Ph.D., Denis Jordan, Ph.D., Vincent Bonhomme, M.D., Rüdiger Ilg, M.D.

ANESTHESIOLOGY 2019; 130:898–911

ABSTRACT

Background: A key feature of the human brain is its capability to adapt flexibly to changing external stimuli. This capability can be eliminated by general anesthesia, a state characterized by unresponsiveness, amnesia, and (most likely) unconsciousness. Previous studies demonstrated decreased connectivity within the thalamus, frontoparietal, and default mode networks during general anesthesia. We hypothesized that these alterations within specific brain networks lead to a change of communication between networks and their temporal dynamics.

Methods: We conducted a pooled spatial independent component analysis of resting-state functional magnetic resonance imaging data obtained from 16 volunteers during propofol and 14 volunteers during sevoflurane general anesthesia that have been previously published. Similar to previous studies, mean z-scores of the resulting spatial maps served as a measure of the activity within a network. Additionally, correlations of associated time courses served as a measure of the connectivity between networks. To analyze the temporal dynamics of between-network connectivity, we computed the correlation matrices during sliding windows of 1 min and applied k-means clustering to the matrices during both general anesthesia and wakefulness.

Results: Within-network activity was decreased in the default mode, attentional, and salience networks during general anesthesia ($P < 0.001$, range of median changes: –0.34, –0.13). Average between-network connectivity was reduced during general anesthesia ($P < 0.001$, median change: –0.031). Distinct between-network connectivity patterns for both wakefulness and general anesthesia were observed irrespective of the anesthetic agent ($P < 0.001$), and there were fewer transitions in between-network connectivity patterns during general anesthesia ($P < 0.001$, median number of transitions during wakefulness: 4 and during general anesthesia: 0).

Conclusions: These results suggest that (1) higher-order brain regions play a crucial role in the generation of specific between-network connectivity patterns and their dynamics, and (2) the capability to interact with external stimuli is represented by complex between-network connectivity patterns.

(ANESTHESIOLOGY 2019; 130:898–911)

EDITOR'S PERSPECTIVE

What We Already Know about This Topic

- The extent to which alterations within specific brain networks impairs communication among networks remains unknown

What This Article Tells Us That Is New

- In a volunteer functional magnetic resonance study, general anesthesia reduced activity within and among networks
- Specific between-network connectivity is necessary for consciousness

The wakeful human is able to flexibly modulate his or her brain activity in order to respond to external stimuli or to execute tasks. These capabilities of the human brain can be eliminated through general anesthesia. As a consequence, anesthetic agents form an experimental framework to investigate the underlying brain physiology.

In the past decade, relevant progress has been made to elucidate the mechanisms of anesthesia-induced unresponsiveness, giving rise to the hypothesis that specific brain regions and the communication between them are necessary to be wakeful. Specifically, changes of connectivity in the default mode network, attentional network, and/or the medial thalamus have been associated with loss of responsiveness during general anesthesia. Electroencephalography analyses have repeatedly shown a significant decrease of frontoparietal information transfer during general anesthesia when compared to wakefulness.[1–3] The underlying

Supplemental Digital Content is available for this article. Direct URL citations appear in the printed text and are available in both the HTML and PDF versions of this article. Links to the digital files are provided in the HTML text of this article on the Journal's Web site (www.anesthesiology.org).

neurophysiologic mechanism of frontoparietal connectivity was further substantiated by functional magnetic resonance imaging experiments that demonstrated a suppression of frontal activation by propofol and subsequently impaired frontoparietal connectivity.[3–5] These observations have been replicated in functional magnetic resonance imaging experiments during sevoflurane-[6,7] and ketamine-induced loss of responsiveness.[8,9] Similarly, dexmedetomidine-induced unresponsiveness was associated with reduced connectivity between the thalamus and the default mode network.[10] In summary, frontoparietal information exchange in the default mode network, the attentional networks, and thalamocortical connectivity to both are thought to be necessary for consciousness. However, there is little knowledge about how changes in few networks lead to a breakdown of between-network communication that we hypothesized to be a neurophysiologic correlate of anesthesia-induced unconsciousness.

One possible explanation is that only a few brain networks are crucial for generating global, dynamic cortical interactions. Indeed, functional magnetic resonance imaging data in humans could demonstrate that "hub" regions exist, characterized by a dominance of long-range connectivity. It is therefore presumed that these regions are capable to dynamically integrate cross-modal information.[11] Additionally, these regions overlap anatomically with the networks affected during general anesthesia. Computational models predicted that lesioning of hub regions is capable of changing long-range connectivity patterns in the human brain.[12–15] Experimentally, it could be demonstrated that anesthesia-induced loss of responsiveness leads to a fragmentation of cortical information processing[16] and to a decreased dynamic repertoire of brain states.[17–19] Taking these results into account, we hypothesized that the altered connectivity of hub regions should result in two observations: (1) decrease of the dynamic repertoire of connectivity patterns under loss of consciousness (irrespective of the anesthetic agent), and (2) the existence of specific dynamic connectivity patterns that can only be observed during consciousness.

To connect prior analyses of within-network activity changes[3,7] with between-network connectivity, we chose a spatial independent component analysis–based approach. We regarded the mean z-score of spatially independent maps or networks as a measure of within-network activity.[7] The correlation matrix of the associated time courses was regarded as a measure of between-network connectivity. Thus, we aimed to model both the modular and intermodular connectivity structure of the human brain. The dynamics of between-network connectivity were modeled with sliding window method calculating the correlation between networks' time courses over 1 min and k-means clustering[20] to identify dominant traits of between-network connectivity patterns (fig. 1).

Submitted for publication June 11, 2018. Accepted for publication February 22, 2019.
From the Department of Neurology (D.G., R.I.), and Department of Anesthesiology (A.R., G.S., D.J.), Klinikum rechts der Isar, Technical University Munich, München, Germany; GIGA-Consciousness, Coma Science Group (S.K.L., C.D.P., S.L.), and GIGA-Consciousness, Sensation and Perception Research Group (A.V., V.B.), GIGA Research, University, and Department of Algology and Palliative Care, Department of Neurology (S.L.), and Department of Anesthesia and Intensive Care Medicine (V.B.), CHU University Hospital of Liège (C.D.P.), Liège, Belgium; GIGA-Cyclotron Research Center: In Vivo Imaging, University of Liège, Liège, Belgium (A.P.); University Department of Anesthesia and Intensive Care Medicine, CHR Citadelle, Liège, Belgium (V.B.); Department of Neurology, University of Wisconsin, Madison, Wisconsin (M.B.); and Asklepios Clinic, Department of Neurology, Bad Tölz, Germany (R.I.).

Materials and Methods

Ethics Statement

The study was conducted in accordance with the Declaration of Helsinki, and the study protocol was approved by the ethics committee of the medical school of the Technical University Munich (Munich, Germany) and the University of Liege (Liege, Belgium), respectively. Applicants to the study were given detailed information about the procedures and potential risks before a written informed consent. All participants were reimbursed for taking part in the study. A medical history was taken from every applicant, especially inquiring about contraindications for general anesthesia using propofol or sevoflurane or examination in a magnetic resonance scanner.

Participants and Anesthesia

The Munich data set included in this analysis has been previously published in Jordan *et al.*[3] and Ranft *et al.*[7] Further details on the study protocol can be found there. Briefly, 15 subjects, aged 21 to 32 yr, were enrolled in the propofol study. For the resting state measurement, participants lay supine in the scanner and were told not to fall asleep while keeping the eyes closed. In the rest of the article, this condition is referred to as "awake." The measurement during propofol-induced loss of responsiveness was carried out using a target-controlled infusion pump (Open TCI; Space infusion system; Braun Medical, Germany). Propofol concentration was increased in 0.4 μg/ml steps beginning at 1.2 μg/ml until volunteers stopped responding to the verbal command "squeeze my hand" (equivalent to a Ramsay sedation scale score of 5 to 6). The concentration was then kept stable for the remaining functional magnetic resonance imaging measurement. This point was reached at plasma concentrations of 2.97 ± 0.47 μg/ml (mean ± SD). Ten minutes of equilibration time passed before the actual measurement took place. Throughout this article, this state as is referred to as propofol-induced loss of responsiveness.

Twenty subjects, aged 20 to 36 yr, were enrolled in the sevoflurane study. The resting state was acquired identical to the propofol setting. Image acquisition during sevoflurane-induced loss of responsiveness was carried out after

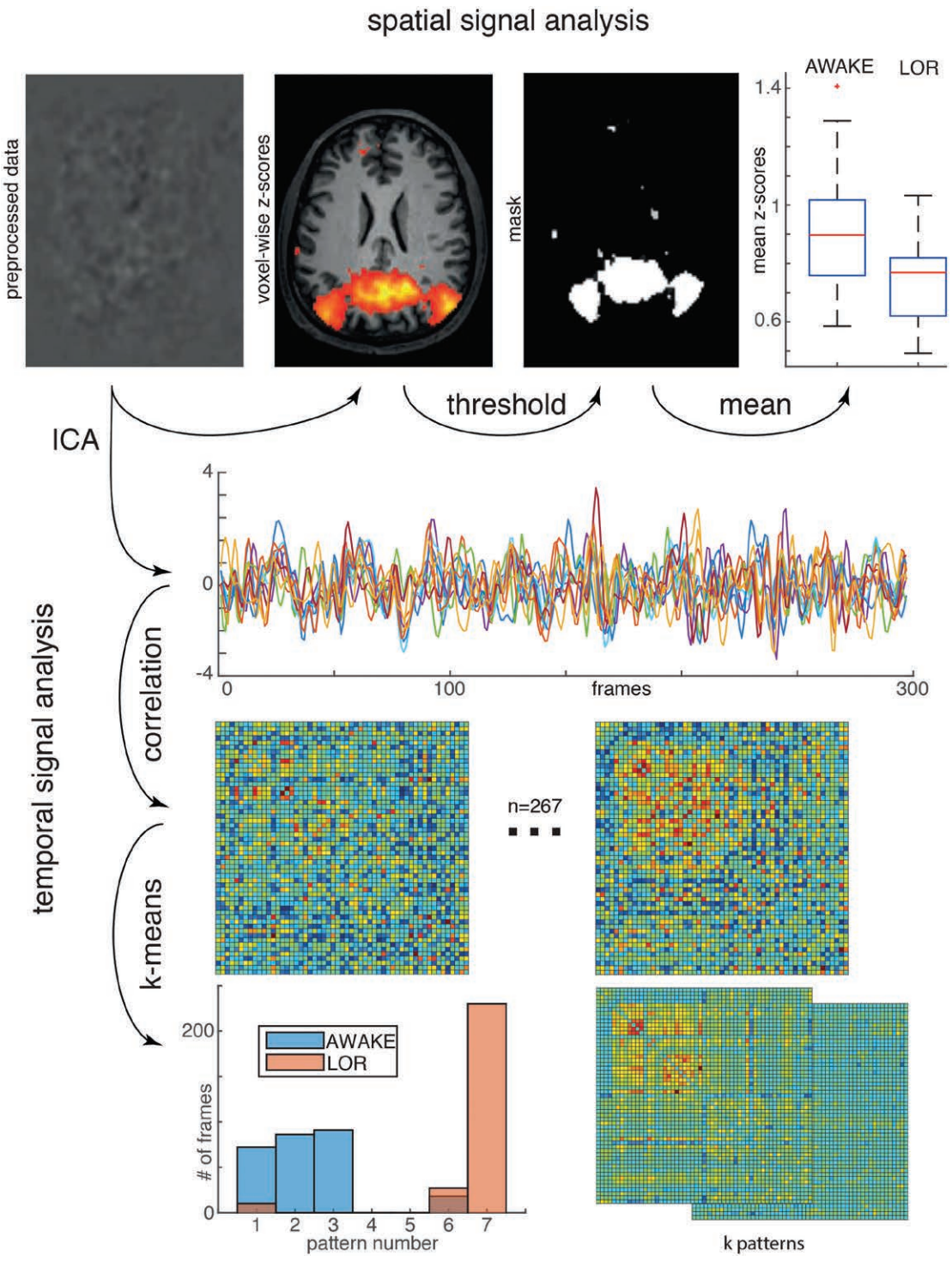

Fig. 1. The flow chart illustrates the spatial and temporal data processing. (*A*) First, a spatial independent component analysis (ICA) decomposed the data into 75 spatially independent components or 56 functional networks and corresponding correlated time courses. In the spatial domain, the components were used to generate masks ($P < 0.001$, uncorrected) and to calculate mean z-scores for each subject and component to quantify the within-network activity. In the temporal domain, the correlation of the individual time courses was calculated in sliding windows of 1 min time. This resulted in 267 correlation matrices per subject and a session of 56 × 56 in size (the number of functional networks). The correlation matrices were regarded as a measure of between-network connectivity and clustered into seven patterns using a k-means algorithm with the sum of the absolute differences (L_1)-distance. LOR, loss of responsiveness.

intubation with a magnetic resonance tomograph-compatible laryngeal mask and during artificial ventilation using an anesthesia machine (Fabius Tiro, Dräger, Germany). Sevoflurane was kept stable at 2 volume percent end-tidal concentration during this condition. Subjects were unresponsive to the command "squeeze my hand" during this condition, tolerated the laryngeal mask well, and showed reduced movements when compared to the wakeful state (see also Ranft *et al.*[7]). It is also noteworthy that clinically this sedation was deeper when compared to propofol-induced loss of responsiveness (corresponding to a Ramsay scale score of 6). In the following we refer to loss of responsiveness irrespective of anesthetic agent as loss of responsiveness. All participants were asked for any memories of the unresponsive state and all reported an amnesia for the procedure.

The Liege data set included in this analysis consisted of 20 subjects during propofol-induced loss of responsiveness. The data was previously published in Boveroux *et al.*[4] From the complete data set (4 men and 16 women, aged 18 to 31 yr), 6 subjects with recording lengths of 300 time points could be included. For anesthesia, propofol was infused through an intravenous catheter placed into a vein of the right arm using a computer-controlled intravenous pump (Alaris TIVA; Carefusion, USA). Subjects were spontaneously breathing throughout the experiment. During the state examined here, propofol-induced loss of responsiveness, subjects were unresponsive to verbal command "squeeze my hand." Clinically, the depth of anesthesia was classified as Ramsay 5. Propofol-induced loss of responsiveness was reached with plasma propofol concentrations of 3.2 ± 0.99 μg/ml (mean ± SD).

Subjects with head motion greater than 2 mm between two subsequent images were excluded from the final analysis. This resulted in 11 datasets from the Munich propofol cohort, 5 subjects from the Liege propofol cohort, and 14 subjects from the sevoflurane cohort.

Functional Magnetic Resonance Imaging Data Acquisition and Preprocessing

Both Munich propofol and sevoflurane image acquisitions were carried out on the same 3-Tesla whole-body magnetic resonance tomographic scanner (Philips Achieva Quasar Dual 3.0T 16CH, The Netherlands) employing an eight-channel, phased-array head coil. Functional magnetic resonance imaging was acquired with a gradient echo planar imaging sequence (echo time = 30 ms, repetition time = 1.838 ms, flip angle = 75°, field of view = 220 × 220 mm^2, matrix = 72 × 72, 32 slices, slice thickness = 3 mm, and 1-mm interslice gap; 300 volumes were acquired in the propofol cohort and 350 volumes were acquired in the sevoflurane cohort; of these 350 frames, the last 50 were discarded). Anatomy was acquired before the functional scan using a single T1-weighted sequence and 1 × 1 × 1-mm voxel size per subject.

The Liege propofol data were acquired on a 3 Tesla Siemens Allegra scanner (Siemens AG, Germany) For the functional magnetic resonance imaging imaging, an Echo Planar Imaging sequence using 32 slices (repetition time = 2,460 ms, echo time = 40 ms, field of view = 220 mm, voxel size = 3.4375 × 3.4375 × 3.9 mm, and matrix size = 64 × 64 × 32) was employed. The individual T1 image was acquired at the end of the whole experiment.

In the following, we describe the analysis steps irrespective of the anesthetic agent, since in this study we were more interested in general mechanisms of loss of responsiveness than in mechanisms of a specific anesthetic agent. The preprocessing was carried out using Statistical Parametric Mapping (SPM12, Wellcome Trust Center for Neuroimaging, University of London, United Kingdom) and Data Processing Assistant for Resting-State fMRI (DPARSF, Release V4.3_170105, State Key Laboratory of Cognitive Neuroscience and Learning, Beijing Normal University, China). We largely followed the parameters in Allen *et al.*[20] in order to make results comparable. Precisely, the first three time points were removed to avoid magnetic coil saturation, slice timing was corrected, and functional images were realigned. Functional images were coregistered to the anatomical image. Six movement parameters and their first derivatives together with five principal components of the white matter and cerebrospinal fluid signal were regressed out, and the data was band-pass filtered between 0.01 to 0.1 Hz. The data was then normalized to Montreal Neurologic Institute space, resliced to a voxel size of 2 × 2 × 2 mm with a third-degree spline interpolation, and smoothed with a 4 × 4 × 4-mm Gaussian kernel.

Functional Magnetic Resonance Imaging Data Analysis

In a first step, the preprocessed functional magnetic resonance imaging data were analyzed using a group level spatial independent component analysis as implemented in the Gift toolbox (Version 4.0b[21]) and GICA3 back reconstruction. The INFOMAX algorithm was employed together with an ICASSO and 20 repetitions to decompose the data into 75 spatially independent components (fig. 1). We preferred this high number of independent components to allow a subdivision of known networks (*e.g.*, the default mode network or its parts) and to be able to analyze both the communication between and within networks, in summary a similar approach to Allen *et al.*[20] We used the GICA3 back reconstruction to generate individual spatial maps and associated (potentially correlated) time courses for each individual map.

This resulted in two types of data: (1) spatially independent components for each subject that were standardized to be standard normally distributed, so-called z-values (we refer to these maps as S_i), and (2) one time course for each component and each subject representing the individual components contribution the overall signal over time. The time courses were also standardized to be standard normally

distributed to account for different scanners and amplitudes of the raw blood oxygenation level dependent signal. We refer to these time courses as R_i.

Both types of data were further analyzed independently with the exception that spatial maps were used to separate networks from noise components. This was necessary since independent component analysis is also known to separate presumable noise from signal of neuronal origin.[22] Signal from neuronal origin was assumed if the component projected on gray matter showed no similarity to venous vessels and if it showed a characteristic frequency spectrum with clear peak less than 0.1 Hz. Noise components usually showed a flat frequency spectrum similar to Gaussian noise. Fifty-six such components with visually high similarity to components in the literature[20,23] were deemed as functional networks and included into the further analysis. This approach is widely used in the literature even though it carries a certain risk to classify neural signal as noise or *vice versa*.

The group level S_i was thresholded at $P < 0.001$, uncorrected in SPM12 to create one mask per functional network. Mean z-scores were then calculated from the single subject, single session back-reconstructed S_i. In the following, we interpret the mean z-values as a measure of activity within a given network and refer to them as "within-network activity."

The time courses R_i were despiked and low-pass filtered less than 0.15 Hz. Correlation matrices were calculated in a sliding window manner identical to Allen *et al.*[20,23] and as implemented in GIFT 4.0b's Temporal dFNC toolbox using 30 time points, equivalent to 1 min, from each measurement, resulting in 267 correlation matrices per measurement (which is 300 recorded volumes minus 3 discarded during preprocessing minus sliding window length). The size of the resulting matrices was 56 × 56, and due to symmetry of the correlation matrices, they contained 56 × 55/2 independent data points. To make correlation matrices more accessible for visual inspection, we sorted the functional network similar to Allen *et al.*[20] in groups, namely basal ganglia networks, auditory networks, somatomotor and somatosensory networks, visual networks, default mode networks, attentional networks, and cerebellar networks. The complete list of networks can be found in the Supplemental Digital Content, http://links.lww.com/ALN/B925. It is noteworthy that this sorting into functional groups has no effect on the later k-means clustering algorithm, since the algorithm only uses the sum of the absolute differences (L_1)-distance of the correlation matrices as a measure of distance and is therefore independent of the order of correlation values. In general, we interpret the correlation values of the networks' time courses as a measure of between-network connectivity and therefore refer to them as "between-network connectivity."

We used the k-means clustering algorithm also implemented in GIFT 4.0b with the L_1-("Manhattan") distance with 20 repetitions to assign the between-network connectivity matrices to between-network connectivity patterns. These patterns are not predefined and are generated by the k-means algorithm as "focal points" or clusters of the between-network connectivity matrices. Only the number of such clusters has to be defined. Since the actual number of clusters k is unknown, we varied the number between k = 2 and k = 10. The results presented in the following are from k = 7 and representative for all k = 2,…, 10 (see also Supplemental Digital Content, http://links.lww.com/ALN/B925).

In order to investigate how information from both within-network activity and between-network connectivity is able to separate wakefulness from unresponsiveness, we formed a summary data matrix containing the within-network activity from the 56 networks together with the absolute number of between-network connectivity pattern appearances in each subject. Due to the high dimensionality (n = 63) and relatively low number of subjects (n = 30), we chose classical Fisher scoring[24] for a prior feature selection. Otherwise the high number of features would make the following analysis prone to overfitting and thus spurious results. Feature selection is a common strategy to reduce dimensionality without missing relevant information. In the analysis presented here, feature selection mainly favors results from within-network activity due to its high number of features (n = 56).[25] This particular Fisher scoring was also chosen because the data matrix contained both normally distributed data (mean z-scores) and sparse data (absolute number of appearances) and because selection of single variables from the data matrix made interpretation of the selection process simpler. After variable ranking, one to five variables were chosen for a support vector machine. For cross-validation, the 30 data sets were randomly divided into 15 training and 15 testing data sets. Single subjects were assigned to either the training or test data set. Since it was not feasible to repeat the process for all partitions of the data set, we repeated the process 1,000 times and averaged across runs. We also conducted the support vector machine with a random permutation of groups of the test data set to illustrate chance level. These steps were carried out with FSLib (Version 5.1, Roffo *et al.*[26]). All analysis steps were carried out in Matlab (R2016a; Mathworks, USA).

Statistical Analysis

Group comparisons were conducted for both the spatial and the temporal domains. Each group contained 30 subjects during awake or loss of responsiveness that were therefore regarded as paired variables.

In the spatial domain, the 75 spatially independent components' mean z-scores were tested for a decrease using the one-sided Mann–Whitney/rank sum test. *P* values were corrected for multiple comparisons using the Bonferroni method (using the multiplicator n = 75; see also Supplemental Digital Content, table 1, http://links.lww.com/ALN/B925).

The supplementary table and the results section give the median change of each component's z-score and the approximated CI using a normal distribution. We chose this approximation since, according to the central limit theorem, the mean of a large number (ranging from 894 to 20,606) of voxels' z-scores is approximately normally distributed.

The number of transitions between the different patterns of between-network connectivity was statistically tested for a difference between awake and loss of responsiveness, propofol-induced loss of responsiveness, and sevoflurane-induced loss of responsiveness using the two-sided Mann–Whitney/rank sum test. The average correlation of the average between-network connectivity matrix was also tested for differences between awake and loss of responsiveness, propofol-induced loss of responsiveness, and sevoflurane-induced loss of responsiveness using the two-sided Mann–Whitney/rank sum test. We chose this test since the actual distribution of the random variables was unknown *a priori*. Differences of pattern distribution between the groups awake, loss of responsiveness, propofol-induced loss of responsiveness, and sevoflurane-induced loss of responsiveness (on the nominal scale of pattern numbers) were tested using a chi-square test with Pearson's chi-square distance.

Results

Our analysis reproduced previous findings about within-network activity changes during loss of responsiveness. More precisely, bilateral ventral and dorsal medial prefrontal cortices (median change, 95% CI: ventral: –0.34 [–0.48; –0.11], dorsal: –0.27 [–0.40; –0.13]), dorsolateral prefrontal cortices (–0.23 [–0.35; –0.091]), the bilateral middle frontal gyruses (–0.17 [–0.31; –0.065]), posterior cingulate cortex and precuneus (–0.31 [–0.42; –0.065]), the right frontoparietal network (–0.18 [–0.34; –0.05]), the bilateral intraparietal (–0.13 [–0.25; –0.049]) cortices, and the salience network (–0.18 [–0.31; –0.044]) showed a significant reduction of within-network activity during loss of responsiveness when compared to awake at a significance level of $P < 0.001$ (Bonferroni-corrected; see Supplemental Digital Content, http://links.lww.com/ALN/B925, for effect sizes and CI of all components). This dominant effect on frontal networks during loss of responsiveness has been shown for both propofol-induced and sevoflurane-induced loss of responsiveness[3,7] as well as significant effects on the medial thalamus only during sevoflurane-induced loss of responsiveness.[6,7] Additionally, loss of responsiveness resulted in a significant decrease of within-network activity in widespread areas at a significance level of $P < 0.05$ (range of change from –0.36 [–0.48; –0.040] in the medial thalamus to –0.10 [–0.33; –0.020] in the bilateral frontal pole). These areas encompass premotor and motor areas, large portions of the parietal lobes and hippocampal network. Within-network activity in the occipital lobes, the temporal lobes, areas around the central sulcus and basal ganglia networks including the thalamus (but not the medial thalamus) were not significantly decreased (range of change from –0.19 [–0.44; 0.063] in the bilateral cuneus to 0.21 [–0.061; 0.42] in the left middle occipital gyrus). In summary, the results replicated previous findings showing a hierarchical and specific effect of anesthesia-induced loss of responsiveness on the brain's networks rather than a uniform decrease of cerebral activity.

The between-network connectivity was modeled with correlation matrices from the independent component's time courses. For visualization of the correlation matrices and increased comparability with other studies, we grouped the 56 functional networks into 7 groups: basal ganglia networks, auditory networks, somatosensory networks, visual network, default mode networks, cognitive control networks, and cerebellar networks (fig. 2, A and B). A complete list of the identified functional networks can be found in the Supplemental Digital Content, http://links.lww.com/ALN/B925. The average between-network connectivity matrix during awake (fig. 2B) showed several remarkable features that have already been described in the previous literature[20]: high between-network connectivity within the groups of somatomotor, visual, and auditory networks and between these groups. Cognitive control networks showed a high between-network connectivity to sensory networks, while some parts of the default mode network also showed low to negative between-network connectivity to these. The average between-network connectivity matrix during loss of responsiveness showed a significant reduction of average between-network connectivity by means of average correlation ($P < 0.001$, median change, 95% CI: –0.031 [–0.058; –0.025], fig. 2C). A differentiated analysis of propofol-induced loss of responsiveness (fig. 2D) and sevoflurane-induced loss of responsiveness (fig. 2E) showed reduction of average between-network connectivity during sevoflurane-induced loss of responsiveness ($P < 0.001$, –0.050 [–0.077; –0.026]) and during propofol-induced loss of responsiveness ($P < 0.05$, –0.023, [–0.057; –0.010]). The between-network connectivity was not significantly smaller during sevoflurane-induced loss of responsiveness when compared to propofol-induced loss of responsiveness ($P = 0.24$, medians, 95% CI: propofol-induced loss of responsiveness: 0.029 [0.022; 0.055], sevoflurane-induced loss of responsiveness: 0.018 [0.016; 0.027]). The visual assessment suggested a decreased between-network connectivity between sensory systems, as well as a less pronounced negative between-network connectivity between cognitive control and default mode networks. Similar observations have successfully been used to distinguish responsive from unresponsive patients[27] and recognized as effects of general anesthesia.[4,8] However, due to the high number of between-network connectivity values in a single matrix and hence unfavorable correction of alpha errors, both observations are not accessible to direct statistical testing

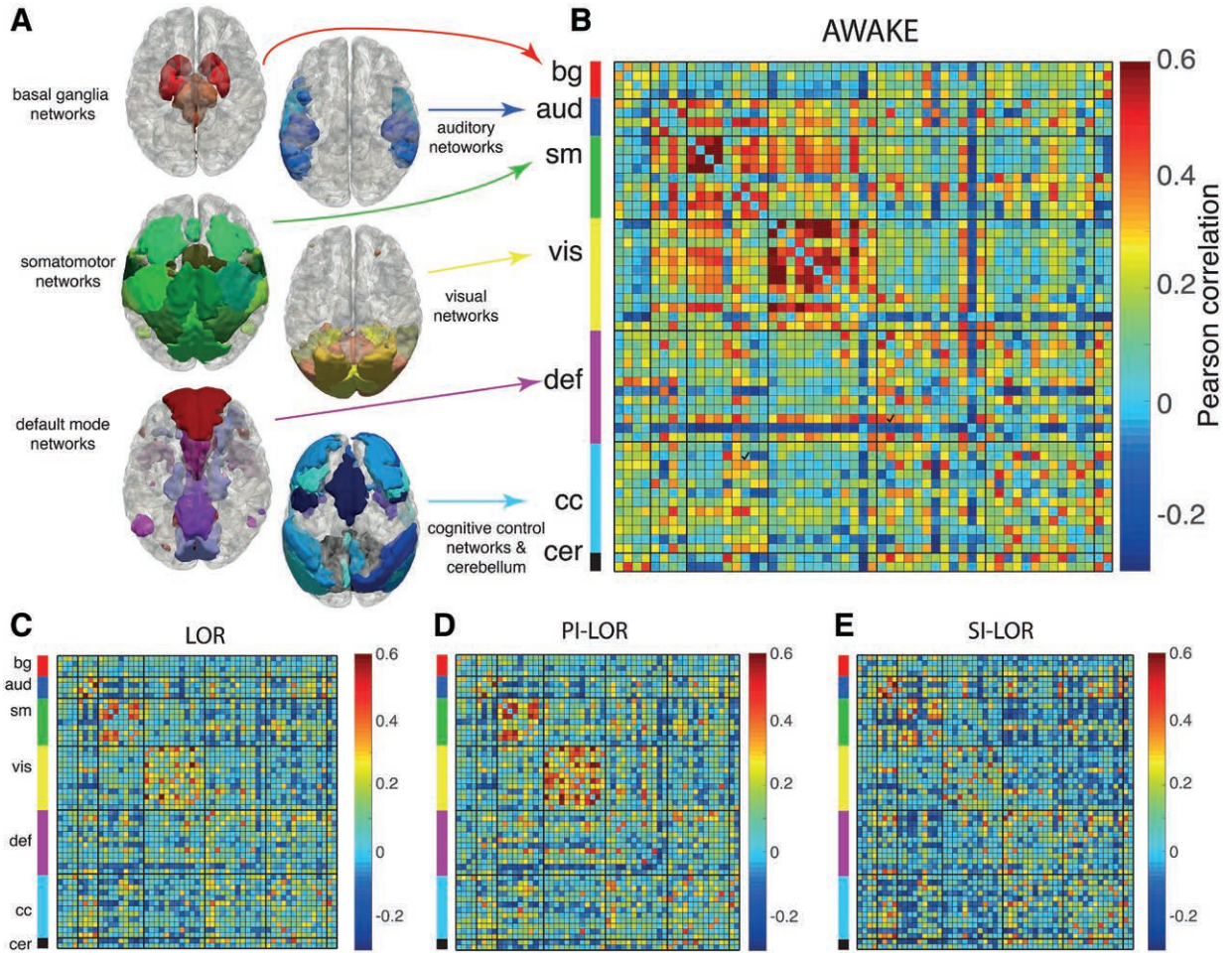

Fig. 2. Average between-network connectivity as assessed by the average correlation between functional networks was significantly decreased during loss of responsiveness (LOR). (*A*) The correlation values of functional networks were sorted into groups of similar behavior: basal ganglia networks, auditory networks, somatomotor networks, default mode networks, cognitive control networks, and cerebellar networks. Note that this rearrangement has no effect on the k-means algorithm and only serves visualization. (*B*) Average between-network connectivity during the "awake" condition (awake refers to the resting state with eyes closed). (*C*) Average between-network connectivity during the LOR condition. (*D*) Average between-network connectivity during propofol-induced loss of responsiveness (PI-LOR). (*E*) Average between-network connectivity during sevoflurane-induced loss of responsiveness (SI-LOR). bg, basal ganglia networks; aud, auditory networks; sm, somatomotor networks; vis, visual networks; def, default mode networks; cc, cognitive control networks; cer, cerebellar networks.

in the framework presented here. Consequently, instead of looking at individual between-network connectivity values, we suggest looking at entire between-network connectivity matrices and interpreting their content as a measure of between-network communication. It is plausible that this between-network connectivity should have characteristic traits and should be subject to dynamic fluctuations that make complex behavior possible in the first place.

We further examined the between-network connectivity matrices using a sliding window method and k-means clustering (see "Materials and Methods" for details) to further quantify the dynamics of between-network connectivity and to isolate characteristic patterns of between-network connectivity. The results are presented for k = 7 in accordance with previous literature,[20] but we also conducted the analyses with k ∈ [2, …, 10] (see Supplemental Digital Content, fig. 1, http://links.lww.com/ALN/B925). The presented results are representative for all examined k. We found that the between-network connectivity patterns and their dynamic change were different during awake and loss of responsiveness. We observed two main findings: (1) during awake, different patterns appeared dynamically (patterns 2, 4, 6, and 7, fig. 3A); and (2) loss of responsiveness was characterized through a dominant pattern of between-network connectivity (pattern 5, fig. 3A). Consequently, the distribution of

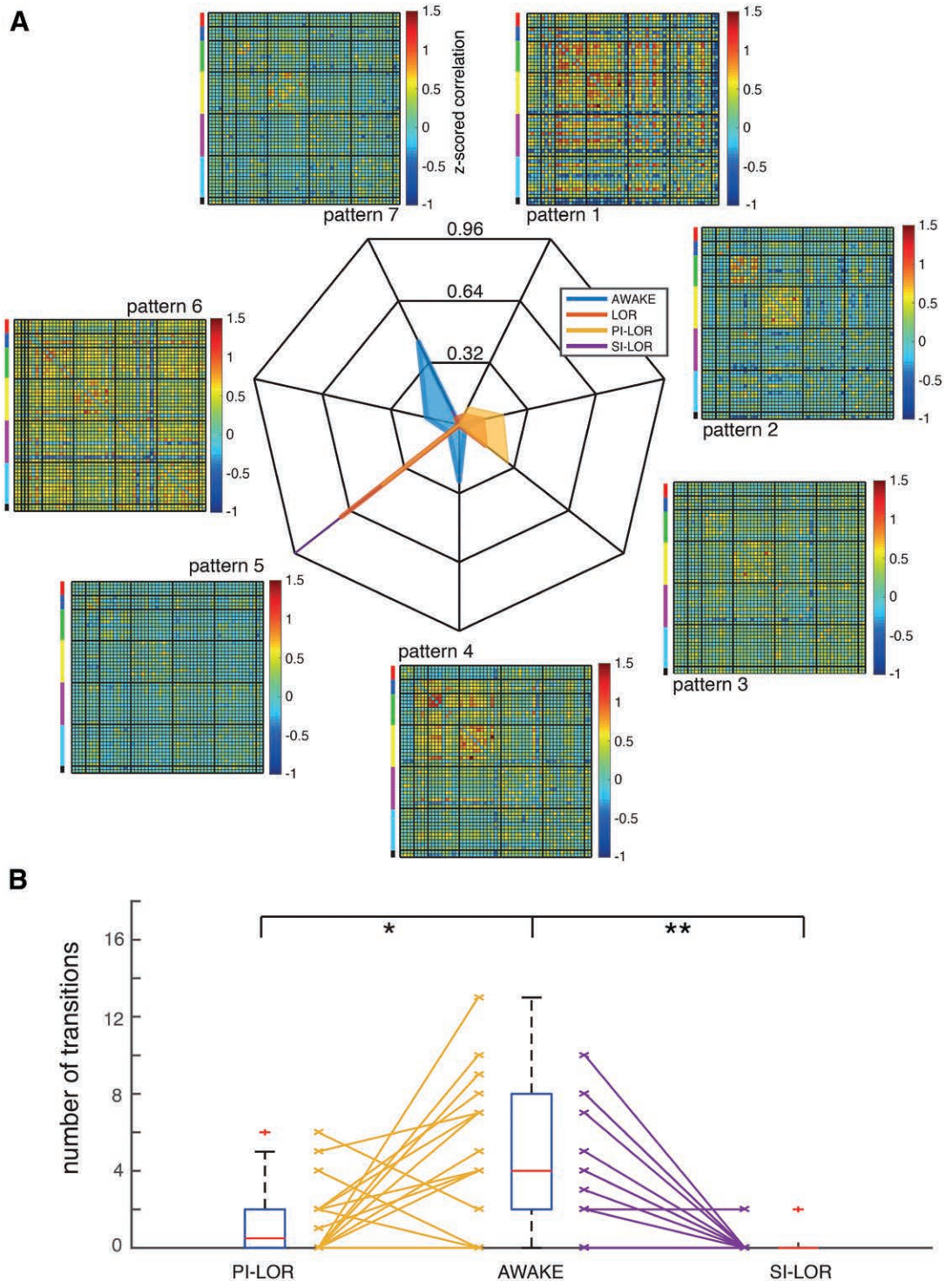

Fig. 3. Loss of responsiveness (LOR) was associated with significantly fewer transitions of between-network connectivity patterns and a significant shift of the between-network connectivity patterns' distribution. (*A*) Radar plot showing the relative number of between-network connectivity matrices assigned to the seven between-network connectivity patterns by the k-means algorithm during AWAKE (*blue*; AWAKE refers to the resting state with eyes closed), LOR (*red*), propofol-induced loss of responsiveness (PI-LOR; *yellow*) and sevoflurane-induced loss of responsiveness (SI-LOR; *purple*). The seven between-network connectivity patterns are shown at different angles of the plot. (*B*) Boxplot showing the absolute number of transitions of between-network connectivity patterns. *Boxes* show medians (*red*) and 25th/75th percentiles. Identical subjects are connected *via lines*. * and **, significant changes during PI-LOR ($P < 0.05$) and SI-LOR ($P < 0.0001$) when compared to AWAKE.

frames across different patterns was significantly different during loss of responsiveness (relative number of pattern appearances: pattern 1: 0.047, pattern 2: 0.11, pattern 3: 0.14, pattern 4: 0.0026, pattern 5: 0.66, pattern 6: 0.0017, pattern 7: 0.031) when compared to awake (relative number of pattern appearances: pattern 1: 0, pattern 2: 0.096, pattern 3: 0.032, pattern 4: 0.25, pattern 5: 0.056, pattern 6: 0.15, pattern 7: 0.42). This was also true for awake *versus* propofol-induced loss of responsiveness (relative number of pattern appearances: pattern 1: 0.089, pattern 2: 0.20, pattern 3: 0.28, pattern 4: 0, pattern 5: 0.43, pattern 6: 0.0033, pattern 7: 0), awake *versus* sevoflurane-induced loss of responsiveness (relative number of pattern appearances: pattern 1: 0, pattern 2: 0, pattern 3: 0, pattern 4: 0.0056, pattern 5: 0.93, pattern 6: 0, pattern 7: 0.066) and propofol-induced loss of responsiveness *versus* sevoflurane-induced loss of responsiveness (all $P < 0.001$). Additionally, we found patterns that occurred exclusively or almost exclusively during loss of responsiveness (numbers 1, 3, and 5) or dominantly during awake (patterns 4, 6, and 7). Among those were one low correlation pattern (7) and two high correlation patterns (4 and 6). Especially pattern 4 showed high similarity with the average correlation matrix. Although patterns 7 and 5 were visually similar, they show a high specificity for either awake or loss of responsiveness.

We regarded the absolute number of transitions between connectivity patterns as a measure of the ongoing dynamics. We found a significant reduction of transitions during loss of responsiveness (median during loss of responsiveness: 0, 95% CI: [0.26; 1.47]) when compared to awake (median during awake: 4, 95% CI: [3.35; 6.12], $P < 0.001$) as well as during propofol-induced loss of responsiveness (median during propofol-induced loss of responsiveness: 0.5, 95% CI: [0.45; 2.55], $P < 0.05$) and sevoflurane-induced loss of responsiveness (median during sevoflurane-induced loss of responsiveness: 0, 95% CI: [–0.17; 0.45], $P < 0.001$, both fig. 3B) when compared to awake. Additionally, the number of transitions was significantly reduced during sevoflurane-induced loss of responsiveness when compared to propofol-induced loss of responsiveness ($P < 0.05$). In total, 27 out 30 subjects showed reduction or no change of transitions during loss of responsiveness when compared to awake. All subjects who had an actual increase of transitions were in the propofol-induced loss of responsiveness group (n = 3, fig. 3B). Thirteen out of 14 subjects of the sevoflurane-induced loss of responsiveness group had 0 transitions during loss of responsiveness, probably reflecting the deeper level of anesthesia during sevoflurane-induced loss of responsiveness when compared to propofol-induced loss of responsiveness. Variation of k € [2, …, 10] also led to a separation into distinct patterns for either the awake or loss of responsiveness state (see Supplemental Digital Content, fig. 1, http://links.lww.com/ALN/B925).

In order to further evaluate the information content of the acquired information about the subject being either in the awake or loss of responsiveness condition, we employed a support vector machine approach after prior feature selection *via* the classical Fisher score.[24] The top five features calculated from the complete data set were appearance of between-network connectivity pattern 5, within-network activity in the dorsal portion of the medial prefrontal cortex, appearance of between-network connectivity pattern 7, within-network activity in the dorsolateral prefrontal cortex, and within-network activity in the ventral portion of the medial prefrontal cortex (fig. 4A). We calculated the accuracy of this classification on the test data with 1, …, 5 top features based on the training data set (fig. 4B) using either within-network activity (mean classification accuracy and 95% CI: 1 feature: 0.72 [0.716; 0.725], 2 features: 0.74 [0.737; 0.745], 3 features: 0.74 [0.738; 0.746], 4 features: 0.75 [0.743; 0.751], 5 features: 0.74 [0.739; 0.747]), between-network connectivity (mean classification accuracy and 95% CI: 1 feature: 0.79 [0.788; 0.793], 2 feature: 0.80 [0.801; 0.808], 3 features: 0.86 [0.858; 0.865], 4 features: 0.90 [0.893; 0.902], 5 features: 0.89 [0.882; 0.893]), both pieces of information (mean classification accuracy and 95% CI: 1 feature: 0.75 [0.742; 0.749], 2 features: 0.82 [0.813; 0.824], 3 features: 0.84 [0.837; 0.847], 4 features: 0.86 [0.850; 0.860], 5 features: 0.87 [0.862; 0.872]), or chance level (mean classification accuracy and 95% CI: 1 feature: 0.50 [0.490; 0.501], 2 features: 0.50 [0.493; 0.504], 3 features: 0.50 [0.494; 0505], 4 features: 0.50 [0.491; 0.502], 5 features: 0.50 [0.490; 0.502]). We observed that both between-network connectivity and the combined data set performed significantly better in terms of accuracy than within-network activity at $P < 0.001$ when compared to a support vector machine-based on within-network activity alone. A significant difference between the combined data set and the between-network connectivity-based support vector machine could be found for 1, …, 5 selected features at $P < 0.05$. In summary, the most important information about discriminating awake from loss of responsiveness was contained in the between-network connectivity patterns 5 and 7 as well as in the within-network activity of the medial prefrontal cortex and the dorsolateral prefrontal cortex. Additionally, the separation between awake and loss of responsiveness using a support vector machine had a significantly higher accuracy using the combined data set or the between-network connectivity patterns when compared to within-network activity in specific networks. All approaches perform significantly better than chance level ($P < 0.001$).

Discussion

Our analyses clearly illustrate the coexistence of effects both in specific networks of the brain and between-network connectivity during anesthesia-induced unconsciousness.

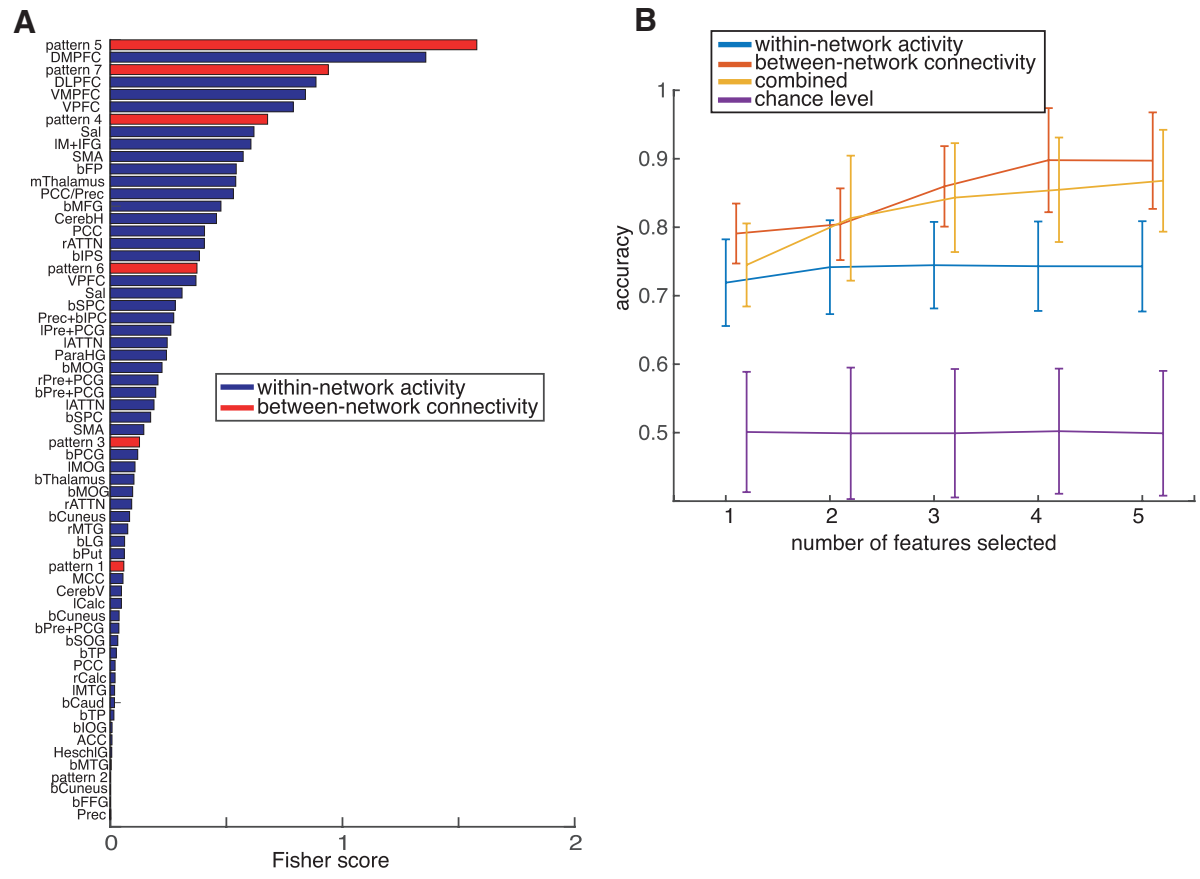

Fig. 4. Appearance of specific between-network connectivity patterns and within-network activity changes in frontal networks and the medial thalamus contains information about the state. (*A*) Barplot showing the absolute Fisher scores and the consequential ranking of features. Within-network activity is shown in *blue*, appearance of between-network connectivity patterns in *red*. (*B*) Performance of a support vector machine differentiating "awake" (awake refers to the resting state with eyes closed) from loss of responsiveness randomly using 50% of the subjects as training data and 50% as test data. Error bar plot shows the mean and SD from 1,000 repetitions based on within-network activity (*blue*), between-network connectivity patterns (*red*), the combined data set (*yellow*), and a random permutation of the test data set, *i.e.*, chance level (*lilac*). The features employed ranged from 1 to 5 according to their respective Fisher score based in the training data. DMPFC, dorsal portion of the medial prefrontal cortex; DLPFC, dorsolateral prefrontal cortex; VMPFC, ventral portion of the medial prefrontal cortex; VPFC, ventromedial prefrontal cortex; Sal, salience network; M+lFG, middle and inferior frontal gyrus; SMA, supplementary motor area; FP, frontal pole; mThalamus, medial thalamus; PCC/Prec, posterior cingulate cortex/ precuneus; MFG, middle frontal gyrus; CerebH, cerebellar hemispheres; ATTN, attentional network/ frontoparietal network; IPS, inferior parietal cortex; SPC, superior parietal cortex; IPC, inferior parietal sulcus; Pre+PCG, pre- and postcentral gyrus; ParaHG, parahippocampal gyrus; MOG, middle occipital gyrus; MTG, middle temporal gyrus; LG, lingual gyrus; Put, putamen; MCC, middle cingulate cortex; CerebV, cerebellar vermis; Calc, calcarine sulcus; SOG, superior temporal gyrus; Caud, caudate nucleus; TP, temporal pole; IOG, inferior occipital gyrus; ACC, anterior cingulate cortex; HeschlG, Heschl's gyrus; FFG, fusiform gyrus. Bilateral/right/left is denoted as preceding b/r/l.

We could demonstrate in line with previous publications on propofol-, sevoflurane-, ketamine-, and dexmedetomidine-induced unconsciousness in humans[3,4,7,8,10] that general anesthesia predominantly affects the within-network activity in the frontal lobe as well as in the medial thalamus during sevoflurane-induced loss of responsiveness.[28] Similar effects have been reported in rodent experiments showing a dominant decrease of connectivity in higher-order brain areas when compared to primary sensory areas during anesthesia.[29] Nevertheless, this finding should not be interpreted as a localized effect of the agent itself. This would not be a plausible explanation since propofol mainly acts by increasing the effect of γ-aminobutyric acid on γ-aminobutyric acid type A receptors,[30] which are known to be widely distributed across the human brain, not only in the above-mentioned brain areas.[31] Similarly, fluranes are thought to affect multiple types of ion channels, potentiate γ-aminobutyric acid–mediated inhibition, increase potassium permeability, and inhibit sodium channels.[32] We therefore propose that a uniform reduction of connectivity in the brain leads to

a disproportionate decrease of within-network activity in specific brain networks whose functioning strongly depends on/results from the tight balancing of incoming excitatory and inhibitor input.

The prominently affected dorsal prefrontal areas have been associated with attentional mechanisms. It has repeatedly been demonstrated that activation in this network is associated with conscious perception and thus reportability of sensory stimuli.[33,34] It has also been proposed in the framework of the global work space theory that the dorsolateral prefrontal cortex might mediate a crucial function: it is supposed to serve as a "bottleneck" for sensory input competing for global distribution in the brain and thus serve both conscious perception and information integration across time and modality.[35] Similarly, both the medial prefrontal cortex's and medial thalamus's connectivity have been repeatedly associated with altered consciousness during general anesthesia.[3,7,8,10,36] It is therefore plausible that these networks form a crucial set of brain regions for intact consciousness. However, it is still conceivable that some of the affected networks are not a necessary requirement, *e.g.*, the cerebellum. Nevertheless, we conclude that at least a subset of the affected networks is required for conscious processing (as assessed by responsiveness).

Additionally, to these hierarchical changes on the cortical level, the subcortically located medial thalamus showed prominently decreased within-network activity during sevoflurane-induced loss of responsiveness. Other studies using functional magnetic resonance imaging,[7] positron emission tomography,[37] or animal models[28] of general anesthesia showed similar results. It is known that the medial thalamus mainly projects to the frontal lobes[38] and is thought to play an important role in the modulation of vigilance.[39] A view that is also backed by the fact that lesioning of the medial thalamus through stroke in humans results in sudden but usually not permanent onset of coma. We conclude that different anesthetic agents have a different mechanisms of action on the network level that nevertheless impair cortical information integration through a common endpoint.

Beyond effects of general anesthesia on specific brain networks, our data clearly show that anesthesia-induced unconsciousness leads to a significant decrease of cortical dynamics irrespective of the investigated agents. This effect led to a shift of the between-network connectivity patterns to only few (propofol-induced loss of responsiveness) or one single pattern (sevoflurane-induced loss of responsiveness) depending on the depth of anesthesia. Similar observations have been made in rat[17] and monkey[19] brains during general anesthesia. Simulation studies of the brain predicted that a general decrease of coupling strength leads to decrease of functional connectivity repertoire.[40] Additionally, it has been predicted that damaging of specific brain regions leads to an overproportionate reduction in the brain's dynamic repertoire.[41] This study clearly demonstrates that both the restriction of functional repertoire and the decrease of activity within functional networks are phenomena associated with loss of responsiveness during general anesthesia, although the causal link between these two phenomena could not be ascertained here. Together with the theoretical predictions made above, we propose that specific brain areas are more important than others to generate a highly dynamic repertoire that is an expression of the wakeful state.

We also want to highlight that specific patterns of between-network connectivity were exclusively observed during wakefulness. These patterns, characterized by high correlation between sensory areas and negative correlation between default mode and attentional networks, have been reported repeatedly.[20,23] The absence of these features has successfully been used to distinguish levels of consciousness in patients with disorders of consciousness,[42] and during general anesthesia.[8] As a consequence, these specific connectivity patterns can be regarded as a modus operandi of the wakeful brain. Similarly, we also observed a pattern of between-network connectivity highly specific for loss of responsiveness. This pattern was characterized by low correlation between functional networks' time courses. This observation has the implication that even though only specific brain networks' within-network activity is significantly diminished, the between-network communication is substantially reduced even between networks that show no significant reduction of within-network activity. Therefore, we conclude that specific brain networks' within-network activity is an important factor influencing between-network communication in distant brain regions.

Of course, the experimental setup and performed analyses presented here have several limitations. It is conceivable that a subset of the effects observed during general anesthesia are unspecific, *i.e.*, changes in brain areas' activity or changes of between-network connectivity patterns might reflect epiphenomena that are independent of the loss of consciousness itself. As an example, we also observed changes in cerebellar within-network activity that are in line with reports of a diminished metabolic rate.[37] However, absence of the cerebellum is not incompatible with consciousness.[43] These unspecific effects might be further emphasized by an increase of the anesthetic agents' concentration beyond the point where loss of responsiveness is actually achieved. From the technical perspective, it is, however, very difficult to obtain functional magnetic resonance imaging data without relevant movement artifacts at this point, a prerequisite for the very complex analysis presented here. In addition, the inclusion of an independent data set from the University of Liege (Liege, Belgium) resulted in stable results both in terms of dynamics of the between-network connectivity and in terms of the patterns encountered. This further underlines that the findings presented here are both reproducible and independent of details of the anesthetic protocol used.

One should also consider that the abstract methodology presented here complicates the interpretation of the

results. Nevertheless, there are several arguments why the mean z-score reflects "within-network activity": (1) mathematically the independent components quantify the spatial extension of the contribution to overall signal, (2) the decrease seen during loss of responsiveness in specific networks is in line with previous experiments using different analytical techniques of functional magnetic resonance imaging data[4,6] or other modalities like positron emission tomography,[37] and (3) independent components classified as artifacts did not show a significant change during loss of responsiveness. Likewise, we propose that the correlation of the associated time courses is a measure of "between-network connectivity" since (1) the time courses represent a measure of the temporal modulation of a given network's contribution to the overall signal, (2) the concept of temporal correlation is a basic principle in functional magnetic resonance imaging to identify functional connectivity, and (3) the encountered patterns have high similarity with patterns from the literature, and the patterns were reproducible in our data set across subjects from different anesthetic protocols and different scanners. In our opinion, the identification of global connectivity patterns that are relevant for consciousness and the concomitant high number of potentially participation brain regions justify this step of data reduction. However, it should also be mentioned that the approach using k-means clustering has one key flaw: the actual alpha error of this step cannot be quantified directly, and hence we encourage any effort to analyze similar data sets using the same method.

Research Support

The Munich experiments were funded by the Departments of Anesthesiology, Neurology, and Neuroradiology of the Klinikum rechts der Isar of the Technical University Munich. The Liege experiments were supported by the Belgian National Funds for Scientific Research (Brussels, Belgium), the European Commission (Brussels, Belgium), the James McDonnell Foundation (Saint Louis, Missouri), the Mind Science Foundation (San Antonio, Texas), the French Speaking Community Concerted Research Action (Brussels, Belgium), the Fondation Medicale Reine Elisabeth (Brussels, Belgium), the University of Liege (Liege, Belgium), and the University Hospital of Liege (Liege, Belgium).

Competing Interests

The authors declare no competing interests.

Correspondence

Address correspondence to Dr. Golkowski: Department of Neurology, Klinikum rechts der Isar, Technical University Munich, Ismaninger Straße 22, 81675 München, Germany. daniel.golkowski@tum.de. Information on purchasing reprints may be found at www.anesthesiology.org or on the masthead page at the beginning of this issue. Anesthesiology's articles are made freely accessible to all readers, for personal use only, 6 months from the cover date of the issue.

References

1. Lee U, Kim S, Noh GJ, Choi BM, Hwang E, Mashour GA: The directionality and functional organization of frontoparietal connectivity during consciousness and anesthesia in humans. Conscious Cogn 2009; 18:1069–78
2. Ku SW, Lee U, Noh GJ, Jun IG, Mashour GA: Preferential inhibition of frontal-to-parietal feedback connectivity is a neurophysiologic correlate of general anesthesia in surgical patients. PLoS One 2011; 6:e25155
3. Jordan D, Ilg R, Riedl V, Schorer A, Grimberg S, Neufang S, Omerovic A, Berger S, Untergehrer G, Preibisch C, Schulz E, Schuster T, Schröter M, Spoormaker V, Zimmer C, Hemmer B, Wohlschläger A, Kochs EF, Schneider G: Simultaneous electroencephalographic and functional magnetic resonance imaging indicate impaired cortical top-down processing in association with anesthetic-induced unconsciousness. Anesthesiology 2013; 119:1031–42
4. Boveroux P, Vanhaudenhuyse A, Bruno MA, Noirhomme Q, Lauwick S, Luxen A, Degueldre C, Plenevaux A, Schnakers C, Phillips C, Brichant JF, Bonhomme V, Maquet P, Greicius MD, Laureys S, Boly M: Breakdown of within- and between-network resting state functional magnetic resonance imaging connectivity during propofol-induced loss of consciousness. Anesthesiology 2010; 113:1038–53
5. Mhuircheartaigh RN, Rosenorn-Lanng D, Wise R, Jbabdi S, Rogers R, Tracey I: Cortical and subcortical connectivity changes during decreasing levels of consciousness in humans: A functional magnetic resonance imaging study using propofol. J Neurosci 2010; 30:9095–102
6. Palanca BJ, Mitra A, Larson-Prior L, Snyder AZ, Avidan MS, Raichle ME: Resting-state functional magnetic resonance imaging correlates of sevoflurane-induced unconsciousness. Anesthesiology 2015; 123:346–56
7. Ranft A, Golkowski D, Kiel T, Riedl V, Kohl P, Rohrer G, Pientka J, Berger S, Thul A, Maurer M, Preibisch C, Zimmer C, Mashour GA, Kochs EF, Jordan D, Ilg R: Neural correlates of sevoflurane-induced unconsciousness identified by simultaneous functional magnetic resonance imaging and electroencephalography. Anesthesiology 2016; 125:861–72
8. Bonhomme V, Vanhaudenhuyse A, Demertzi A, Bruno MA, Jaquet O, Bahri MA, Plenevaux A, Boly M, Boveroux P, Soddu A, Brichant JF, Maquet P, Laureys S: Resting-state network-specific breakdown of

functional connectivity during ketamine alteration of consciousness in volunteers. Anesthesiology 2016; 125:873–88
9. Lee U, Ku S, Noh G, Baek S, Choi B, Mashour GA: Disruption of frontal-parietal communication by ketamine, propofol, and sevoflurane. Anesthesiology 2013; 118:1264–75
10. Akeju O, Loggia ML, Catana C, Pavone KJ, Vazquez R, Rhee J, Contreras Ramirez V, Chonde DB, Izquierdo-Garcia D, Arabasz G, Hsu S, Habeeb K, Hooker JM, Napadow V, Brown EN, Purdon PL: Disruption of thalamic functional connectivity is a neural correlate of dexmedetomidine-induced unconsciousness. Elife 2014; 3:e04499
11. van den Heuvel MP, Sporns O: Rich-club organization of the human connectome. J Neurosci 2011; 31:15775–86
12. Váša F, Shanahan M, Hellyer PJ, Scott G, Cabral J, Leech R: Effects of lesions on synchrony and metastability in cortical networks. Neuroimage 2015; 118:456–67
13. Alstott J, Breakspear M, Hagmann P, Cammoun L, Sporns O: Modeling the impact of lesions in the human brain. PLoS Comput Biol 2009; 5:e1000408
14. Gratton C, Nomura EM, Pérez F, D'Esposito M: Focal brain lesions to critical locations cause widespread disruption of the modular organization of the brain. J Cogn Neurosci 2012; 24:1275–85
15. Moon JY, Lee U, Blain-Moraes S, Mashour GA: General relationship of global topology, local dynamics, and directionality in large-scale brain networks. PLoS Comput Biol 2015; 11:e1004225
16. Schröter MS, Spoormaker VI, Schorer A, Wohlschläger A, Czisch M, Kochs EF, Zimmer C, Hemmer B, Schneider G, Jordan D, Ilg R: Spatiotemporal reconfiguration of large-scale brain functional networks during propofol-induced loss of consciousness. J Neurosci 2012; 32:12832–40
17. Hudetz AG, Liu X, Pillay S: Dynamic repertoire of intrinsic brain states is reduced in propofol-induced unconsciousness. Brain Connect 2015; 5:10–22
18. Hutchison RM, Hutchison M, Manning KY, Menon RS, Everling S: Isoflurane induces dose-dependent alterations in the cortical connectivity profiles and dynamic properties of the brain's functional architecture. Hum Brain Mapp 2014; 35:5754–75
19. Barttfeld P, Uhrig L, Sitt JD, Sigman M, Jarraya B, Dehaene S: Signature of consciousness in the dynamics of resting-state brain activity. Proc Natl Acad Sci USA 2015; 112:887–92
20. Allen EA, Damaraju E, Plis SM, Erhardt EB, Eichele T, Calhoun VD: Tracking whole-brain connectivity dynamics in the resting state. Cereb Cortex 2014; 24:663–76
21. Calhoun V: GroupICATv4.0b, 2017. Available at: http://mialab.mrn.org/software/gift/#. Accessed April 14, 2019
22. Correa N, Adali T, Calhoun VD: Performance of blind source separation algorithms for fMRI analysis using a group ICA method. Magn Reson Imaging 2007; 25:684–94
23. Allen EA, Erhardt EB, Damaraju E, Gruner W, Segall JM, Silva RF, Havlicek M, Rachakonda S, Fries J, Kalyanam R, Michael AM, Caprihan A, Turner JA, Eichele T, Adelsheim S, Bryan AD, Bustillo J, Clark VP, Feldstein Ewing SW, Filbey F, Ford CC, Hutchison K, Jung RE, Kiehl KA, Kodituwakku P, Komesu YM, Mayer AR, Pearlson GD, Phillips JP, Sadek JR, Stevens M, Teuscher U, Thoma RJ, Calhoun VD: A baseline for the multivariate comparison of resting-state networks. Front Syst Neurosci 2011; 5:2
24. Gu Q, Li Z, Han J: Generalized Fisher score for feature selection. arXiv preprint arXiv:1202.3725, 2012 .Available at: https://arxiv.org/ftp/arxiv/papers/1202/1202.3725.pdf. Accessed April 14, 2019
25. Frohlich H, Chapelle O, Scholkopf B: Feature selection for support vector machines by means of genetic algorithm, tools with artificial intelligence, 2003. Proceedings. 15th ieee international conference on, IEEE, 2003, pp 142–148. Available at: https://www.researchgate.net/profile/Holger_Froehlich2/publication/221417489_Feature_Selection_for_Support_Vector_Machines_by_Means_of_Genetic_Algorithms/links/0deec53c66ef1ad803000000.pdf. Accessed April 14, 2019
26. Roffo G, Melzi S, Castellani U, Vinciarelli A: Infinite latent feature selection: A probabilistic latent graph-based ranking approach. arXiv preprint arXiv:1707.07538, 2017. Available at: http://openaccess.thecvf.com/content_ICCV_2017/papers/Roffo_Infinite_Latent_Feature_ICCV_2017_paper.pdf. Accessed April 14, 2019
27. Demertzi A, Antonopoulos G, Heine L, Voss HU, Crone JS, de Los Angeles C, Bahri MA, Di Perri C, Vanhaudenhuyse A, Charland-Verville V, Kronbichler M, Trinka E, Phillips C, Gomez F, Tshibanda L, Soddu A, Schiff ND, Whitfield-Gabrieli S, Laureys S: Intrinsic functional connectivity differentiates minimally conscious from unresponsive patients. Brain 2015; 138(pt 9):2619–31
28. Alkire MT, McReynolds JR, Hahn EL, Trivedi AN: Thalamic microinjection of nicotine reverses sevoflurane-induced loss of righting reflex in the rat. Anesthesiology 2007; 107:264–72
29. Liang Z, Liu X, Zhang N: Dynamic resting state functional connectivity in awake and anesthetized rodents. Neuroimage 2015; 104:89–99
30. Franks NP: General anaesthesia: From molecular targets to neuronal pathways of sleep and arousal. Nat Rev Neurosci 2008; 9:370–86
31. Persson A, d'Argy R, Gillberg PG, Halldin C, Litton JE, Swahn CG, Sedvall G: Autoradiography with saturation

experiments of 11C-Ro 15-1788 binding to human brain sections. J Neurosci Methods 1991; 36:53–61
32. Antkowiak B: How do general anaesthetics work? Naturwissenschaften 2001; 88:201–13
33. Dehaene S, Changeux JP: Experimental and theoretical approaches to conscious processing. Neuron 2011; 70:200–27
34. van Vugt B, Dagnino B, Vartak D, Safaai H, Panzeri S, Dehaene S, Roelfsema PR: The threshold for conscious report: Signal loss and response bias in visual and frontal cortex. Science 2018; 360:537–42
35. Dehaene S, Sergent C, Changeux JP: A neuronal network model linking subjective reports and objective physiological data during conscious perception. Proc Natl Acad Sci USA 2003; 100:8520–5
36. Pal D, Dean JG, Liu T, Li D, Watson CJ, Hudetz AG, Mashour GA: Differential role of prefrontal and parietal cortices in controlling level of consciousness. Curr Biol 2018; 28:2145–2152.e5
37. Kaisti KK, Långsjö JW, Aalto S, Oikonen V, Sipilä H, Teräs M, Hinkka S, Metsähonkala L, Scheinin H: Effects of sevoflurane, propofol, and adjunct nitrous oxide on regional cerebral blood flow, oxygen consumption, and blood volume in humans. Anesthesiology 2003; 99:603–13
38. Behrens TE, Johansen-Berg H, Woolrich MW, Smith SM, Wheeler-Kingshott CA, Boulby PA, Barker GJ, Sillery EL, Sheehan K, Ciccarelli O, Thompson AJ, Brady JM, Matthews PM: Non-invasive mapping of connections between human thalamus and cortex using diffusion imaging. Nat Neurosci 2003; 6:750–7
39. Liu X, Lauer KK, Ward BD, Li SJ, Hudetz AG: Differential effects of deep sedation with propofol on the specific and nonspecific thalamocortical systems: A functional magnetic resonance imaging study. Anesthesiology 2013; 118:59–69
40. Deco G, Kringelbach ML: Metastability and coherence: Extending the communication through coherence hypothesis using a whole-brain computational perspective. Trends Neurosci 2016; 39:125–35
41. Deco G, Van Hartevelt TJ, Fernandes HM, Stevner A, Kringelbach ML: The most relevant human brain regions for functional connectivity: Evidence for a dynamical workspace of binding nodes from whole-brain computational modelling. Neuroimage 2017; 146:197–210
42. Di Perri C, Amico E, Heine L, Annen J, Martial C, Larroque SK, Soddu A, Marinazzo D, Laureys S: Multifaceted brain networks reconfiguration in disorders of consciousness uncovered by co-activation patterns. Hum Brain Mapp 2018; 39:89–103
43. Lemon RN, Edgley SA: Life without a cerebellum. Brain 2010; 133(pt 3):652–4